  Bull. Chem. Soc. Jpn., 61, 199—205 (1988)

Photoacoustic Study of 280 nm Band of Acetone Vapor

Takefumi OKA,* Humiyo KOBAYASHI, Naoki OGUMA, and Makoto MOROHASHI
Department of Electrical Engineering, Nagaoka Technical College, 888 Nishikatakai Nagaoka, Niigata 940
(Received June 8, 1987)

Relaxation of the energy absorbed by acetone vapor (200 Torr) on excitation with UV (230—340 nm) was investigated by the photoacoustic technique. The presence of two relaxation paths was found by their difference in heat production rates: The faster path is $S_0 \rightarrow S_1 \rightarrow T_1 \rightarrow S_0$ and the slower path is $S_0 \rightarrow$ radicals→recombination products. The PA spectra corresponding to these paths were determined separately. The spectrum for the T_1 path has a peak around 295 nm and extends to longer wavelengths beyond 310 nm. The spectrum for the decomposition path has a peak around 275 nm and overlaps with the spectrum for the T_1 path in the region of $\lambda<310$ nm. The study of frequency dependences of PA signals showed the presence of faster and slower heat releasing steps in each path. In the T_1 path, the faster and the slower steps are due to vibrational deactivation of hot T_1 formed from S_1 and of hot S_0 formed from T_1 respectively. In the radical path, the faster and slower steps are the deactivation of the hot radicals and the recombination of the thermalized radicals respectively. The addition of O_2 to the system accelerated the heat release process via the relaxed T_1 and also converted the slow heat release process of recombination into a fast process of addition reactions of O_2 to the radicals.

When a gas in a closed space is irradiated with intensity modulated radiation, generally some of the energy absorbed is released as modulated heat. This in turn produces a modulated pressure change, an acoustic wave. This is known as Photo Acoustic Effect (PA hereafter).

The frequency of the PA signal is the same as that of the excitation radiation but the PA signal has a phase lag behind the radiation. The phase lag as well as the amplitude of the PA signal bears information about the relaxation of the absorbed energy to heat.

By comparison of in-phase and out-of-phase PA spectra which are observed at phase angles separated by 90°, we can distinguish parts of an absorption band relaxing at different rates. Biacetyl,[1] azabenzenes,[2] and aromatic ketones[3] have been studied in this way. If the PA spectrum and the absorption spectrum of a particular gas are different, it also indicates the presence of different relaxation processes in that absorption band. This kind of technique has been used to determine the fluorescence quantum yield of benzene[4] and to investigate nonradiative processes of benzene.[5]

The frequency dependence of the phase lag provides chance to determine the rate constant of the relaxation process involved. Hunter et al. have developed a multi-state relaxation model[6] and have determined the triplet lifetimes of biacetyl,[7] benzenes,[8] and alkyl iodides[9,10] by applying the model to the frequency dependence of phase lag and/or amplitude.

In the present study, acetone is investigated by the PA technique measuring the PA spectra and the frequency dependence of the phase lag.

Acetone has an absorption band ranging from 220 nm to 330 nm with a maximum around 275 nm. The fluorescence quantum yield is very low (<0.002)[11] and nonradiative processes dominate the decay process. For low vibrational levels of S_1, the quantum yield of the $S_1 \rightarrow T_1$ intersystem crossing is 1 and $k_{isc}=3.8\times10^8\ s^{-1}$.[12] The intersystem crossing $S_1 \rightarrow T_1$ should form a hot triplet. On decreasing the excitation wavelength below 310 nm, k_{isc} decreases but the decomposition rate constant k_d increases.[13] Recently, Copeland and Crosley have reported the barrier height for decomposition into CH_3 and $COCH_3$ to be 385 kJ mol^{-1} above the ground state S_0 (50 kJ mol^{-1} above T_1). They have also shown the vibrational deactivation rate constant of the hot triplet by S_0 to be 7.59×10^{10} mol^{-1} dm^3 s^{-1} ($\approx10^9$ s^{-1} with 200 Torr of acetone (1 Torr=133.322 Pa)) and the lifetime of the thermal triplet to be 0.225 ms.[14] Since the quantum yield of the phosphorescence is small (≈0.02),[15] the lifetime of T_1 is ascribed to intersystem crossing to S_0.

Therefore we expect two paths of heat production in acetone: fast heat ($\approx50+\alpha$ kJ mol^{-1}) followed by slow ($\tau\approx0.2$ ms) heat (≈335 kJ mol^{-1}) for the $S_0 \rightarrow S_1 \rightarrow T_1 \rightarrow S_0$ path and fast heat ($\approx50+\alpha$ kJ mol^{-1}) followed by very slow heat (≈335 kJ mol^{-1})[16] for the $S_0 \rightarrow$ radicals→recombination products path. The α depends on the excess energy above the barrier. T_1 is quenched by oxygen with the rate constant of 8.4×10^9 mol^{-1} dm^3 s^{-1} (5×10^7 s^{-1} with 100 Torr of O_2). Consequently the rate of heat production due to T_1 should increase in the presence of O_2.

Method

In order to analyze the PA spectra and the frequency dependence of the phase lag, equations to describe them are derived below. We assume a sinusoidally amplitude modulated light beam:

$$I(\lambda) = I_0(\lambda)(\delta+\sin\omega t)$$

where $I_0(\lambda)$ is the beam intensity at a wavelength of λ, ω is the angular frequency of modulation and δ is the relative intensity of the DC component. The light absorption process is expressed as

$$S_0 + h\nu \xrightarrow{I(\lambda)A(\lambda)} S_1$$

where $A(\lambda)$ is the fraction of the absorption over the full path length divided by the path length, and S_0 and S_1 refer to the ground and excited state respectively.

First, we shall deal with the PA spectra for a system which has two heat production processes with different rate constants. We assume two paths for heat production characterized by $\{r_1(\lambda), X_1, k_1, q_1\}$ and $\{r_2(\lambda), X_2, k_2, q_2\}$ as shown in the equations below.

$$S_1 \xrightarrow{r_1(\lambda)} X_1 \xrightarrow{k_1} S_0 + q_1$$
$$S_1 \xrightarrow{r_2(\lambda)} X_2 \xrightarrow{k_2} S_0 + q_2$$

where r_1 and r_2 refer to branching ratios from S_1 to the states X_1 and X_2 respectively, and X_1 and X_2 are only symbolic. They may or may not be real states. The point is that there are two parallel processes producing heat q_1 with a rate constant k_1 and heat q_2 with k_2. The heat production process may not be a single step in each path, but we assume so here. This assumption is adequate for the purpose of spectral analysis. Later we will employ a two-step model for the analysis of the frequency dependence.

The acoustic pressure $p(t)$ expected for the above scheme is as follows.

$$p(t) = K\frac{I_0(\lambda)}{\sqrt{\omega^2+k_t^2}}\{A_1(\lambda)b_1(\omega)\sin(\omega t-\phi_a-\phi_1) + A_2(\lambda)b_2(\omega)\sin(\omega t-\phi_a-\phi_2)\}$$

where $A_i(\lambda)=A(\lambda)r_i/(r_1+r_2)$, $b_i(\omega)=k_iq_i/\sqrt{\omega^2+k_i^2}$, $\phi_i=\tan^{-1}(\omega/k_i)$, k_t is a reciprocal of the time of thermal relaxation of the heated gas onto the cell walls and ϕ_a represents a phase lag due to the apparatus including a phase lag due to a thermal diffusivity effect. K is a constant independent of t, ω, and λ.

Then, the output of a lock-in amplifier $p(\lambda)$ is

$$p(\lambda) = K\frac{I_0(\lambda)}{\sqrt{\omega^2+k_t^2}}\{A_1(\lambda)b_1(\omega)\cos(\phi_r-\phi_a-\phi_1) + A_2(\lambda)b_2(\omega)\cos(\phi_r-\phi_a-\phi_2)\} \quad (1)$$

where ϕ_r is an adjustable phase lag of a reference signal. The in-phase spectrum with respect to the heat q_1 can be obtained by setting $\phi_r=\phi_a+\phi_1$:

$$p_{in}(\lambda) = K\frac{I_0(\lambda)}{\sqrt{\omega^2+k_t^2}}\{A_1(\lambda)b_1(\omega) + A_2(\lambda)b_2(\omega)\cos(\phi_1-\phi_2)\}. \quad (2)$$

The out-of-phase spectrum is given by setting $\phi_r=\phi_a+\phi_1+90°$ as

$$p_{out}(\lambda) = K\frac{I_0(\lambda)}{\sqrt{\omega^2+k_t^2}}\{0-A_2(\lambda)b_2(\omega)\sin(\phi_1-\phi_2)\}. \quad (3)$$

Since we know the shape of $I_0(\lambda)$ from a PA spectrum of carbon black,[18] the shape of the spectrum $A_2(\lambda)$ can be obtained from the out-of-phase spectrum of Eq. 3. Generally, the other spectrum $A_1(\lambda)$ can not be determined from $p_{in}(\lambda)$ of Eq. 2 even if the shape of $A_2(\lambda)$ is known. In the present study, however, we can find the shape of $A_1(\lambda)$ because $A_2(\lambda)b_2(\omega)$ term in $p_{in}(\lambda)$ is negligibly small compared to $A_1(\lambda)b_1(\omega)$ at particular frequencies.

Next we shall deal with the frequency dependence of the PA signal. In the spectrum analysis (Eqs. 1—3), we assumed for simplicity a single step, and consequently one rate constant for each heat producing path. The frequency analysis is only effective for a single path mechanism. Usually, a real path has many steps in series.

Here we assume a single path model consisting of two steps in series which are characterized by different rate constants as shown in Fig. 1. This model is essentially the same as the one used by Hunter et al.[6] In the first step, the fast heat F is released with a rate constant of $1/\tau_f$ and the slow heat S is released with a rate constant of $1/\tau_s$ in the second step.

When $\tau_f \ll \tau_s$, the PA signal can be approximated by

$$p(t) = K\frac{I_0(\lambda)}{\sqrt{\omega^2+k_t^2}}A(\lambda)b(\omega)\sin(\omega t-\phi_a-\phi) \quad (4)$$

where

$$b(\omega) = S\sqrt{(F/S)^2+\{1+2(F/S)\}/\{1+(\omega\tau_s)^2\}} \quad (5)$$

$$\phi = \mathrm{Tan}^{-1}\frac{\omega\tau_s}{(F/S)\{1+(\omega\tau_s)^2\}+1} \quad (6)$$

ϕ_a: a phase lag of the apparatus including that due to the thermal diffusivity effect. The $b(\omega)$ can be interpreted as the effective heat detected at ω. If this two-step model is applicable to each path in the previous model for spectral analysis, then the $b_i(\omega)$ terms in Eqs. 1—3 must be replaced by $b(\omega)$ of Eq. 5. Of course, S, F, and τ_s are different for each path.

To use frequency dependence of the PA amplitude, a logarithmic function of the amplitude, excluding the thermal diffusivity factor, is useful:

$$\log\{b(\omega)/S\} = \frac{1}{2}\log\left\{(F/S)^2+\frac{1+2(F/S)}{1+(\omega\tau_s)^2}\right\}. \quad (7)$$

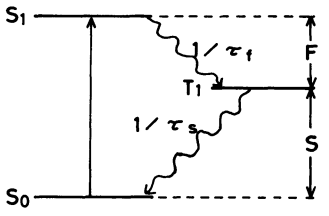

Fig. 1. A model of a relaxation path consisting of two steps in series. τ_f and F refer to the lifetime and the heat released in the first(fast) step; τ_s and S those in the second (slow) step. T_1 is not necessarily a triplet state and can be any state.

This quantity decreases as the frequency increases. The limiting values at lower frequencies and at higher frequencies are $\log\{1+(F/S)\}$ and $\log(F/S)$ respectively. Therefore we can determine the ratio of the fast heat(F) to the slow heat(S) if the relative amplitudes are obtained over a wide frequency range.

The phase lag ϕ is a more sensitive function of ω than the amplitude. To extract information on the relaxation due to the sample gas from the experimentally observed phase lag ($\phi+\phi_a$), ϕ_a must be determined and be subtracted. This can be done using a gas which has no slow heat, i.e. $S=0$ and consequently no phase lag, i.e. $\phi=0$. With this gas the observed phase lag is equal to ϕ_a.

The function ϕ of Eq. 6 has a maximum of $\tan^{-1}\frac{1}{2\sqrt{(F/S)\{1+(F/S)\}}}$ at $\omega=\{1+(S/F)\}/\tau_s$ and takes small values at lower and higher frequencies. When we observed this maximum, we can determine both the ratio F/S and the lifetime τ_s.

Experimental

The apparatus used is schematically shown in Fig. 2. The light source was a 500W xenon arc lamp (Ushio, UXL500D). The light beam was modulated at a frequency between 10 and 1000 Hz by a rotating disk chopper (Scetic Instruments, 300C) and then was passed through a 20 cm scanning monochromator (Ritsu, MC-20L) with a bandpass of 4.2 nm. The modulated monochromatic light beam was passed through a cylindrical PA cell (18 mm diameter, 70 mm long) along its axis to a solar blind phototube (HTV R1384).

The body of the PA cell was made of Pyrex, and two quartz windows were attached to the cell with epoxy resin. This cell also had two gas ports with greaseless stop cocks. PA signals were sensed by an electret microphone with a built-in FET preamplifier. The microphone was mounted in a small cavity adjacent to the cell body at its middle by using electron wax. The back side of the microphone was sealed with epoxy resin to make it vacuum tight. The microphone was polarized by a battery (9 V).

The output of the microphone (or of the phototube) was sent to a lock-in amplifier (Stanford Research Inc., SR 510) where a signal from a photocoupler on the chopper was used as a reference signal. The output of the lock-in amplifier was fed into a strip chart recorder.

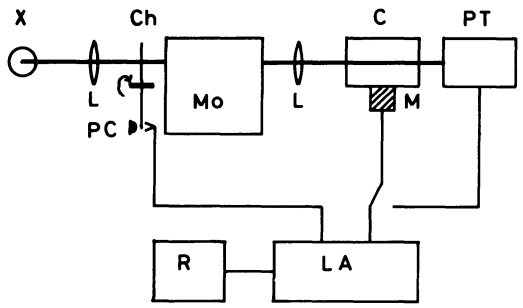

Fig. 2. Block diagram of the apparatus.
X, Xe lamp; L, lens; Ch, chopper; Mo, monochromator; C, cell; M, microphone; PT, photo tube; PC, photo coupler; LA, lock-in amplifier; R, recorder.

Sample gases were mixtures of acetone 200 Torr and a buffer gas (Ar or air) 560 Torr. The cell was filled on a conventional vacuum line. Filling and pumping of the cell was done slowly ($\approx$1 Torr s^{-1}) to prevent rupturing the diaphragm of the microphone.

To test the performance of this cell, measurements were made on mixtures of benzene vapor and a buffer gas (Ar or air). The cell showed no resonance below 1.5 kHz. The phase lag obtained with the mixtures showed chopping frequency dependence, but this was used as a phase lag of the apparatus (ϕ_a in Eq. 4).

To obtain corrected PA spectra, apparent PA spectra were divided by a PA spectrum of carbon black.[18] The spectra in Figs. 5, 9, and 10 are so corrected.

Three kinds of measurements were done in the present work.

1. PA spectra were measured by scanning the wavelength with a fixed chopping frequency at two fixed phase angles separated by 90° from each other.
2. The frequency dependence of the phase lag was obtained by a null reading at various chopping frequencies between 10 and 1000 Hz at a fixed wavelength.
3. Optical absorption spectra were obtained by division of a spectrum of the transmitted light intensity with a sample gas mixture in the cell by that with a buffer gas alone.

All the measurements were done at room temperature.

Results and Discussion

PA Spectra in Ar. The PA spectra of acetone (200 Torr) with Ar as a buffer gas at a frequency of 20 Hz are shown in Fig. 3. The out-of-phase spectrum (ϕ=90° in Fig. 3) was taken with the phase angle to null PA signal at 310 nm. The in-phase spectrum (ϕ=0°) was taken with a phase lead of 90° in front of the phase angle of the out-of-phase spectrum. At wavelengths longer than 310 nm, the signal appears

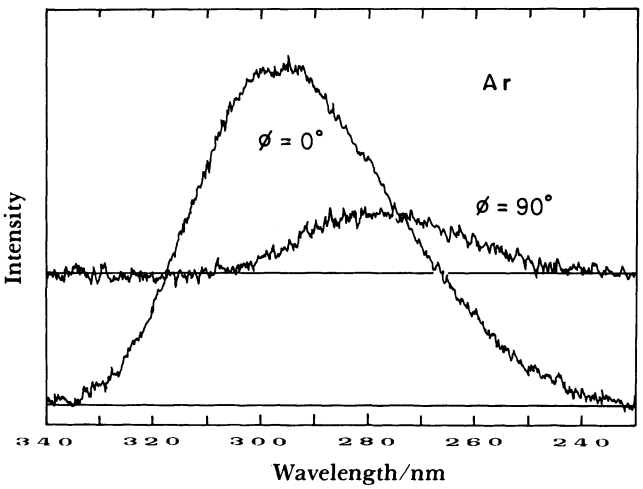

Fig. 3. PA spectra of acetone with Ar as a buffer gas (f=20 Hz). Acetone 200 Torr and Ar 560 Torr. Phase angles are of relative values.

only in the in-phase spectrum. This means that at $\lambda>310$ nm, there is only one relaxation process. On the other hand, there are two processes at $\lambda<310$ nm. In other words, the situation of Eqs. 2 and 3 is achieved in Fig. 3; Eq. 2 corresponds to the in-phase spectrum in the figure and Eq. 3 to the out-of-phase spectrum. The out-of-phase spectrum represents the spectral shape of one ($I_0(\lambda)A_2(\lambda)$ in Eq. 3) of two relaxation processes, which is a relatively slower one because the positive value of the out-of-phase spectrum results in $\phi_2>\phi_1$ in Eq. 3.

According to Eq. 2, the in-phase spectrum should be a mixture of two spectra $I_0(\lambda)A_2(\lambda)$ and $I_0(\lambda)A_1(\lambda)$. To confirm this interpretation, we examined the PA spectra at various frequencies (20—700 Hz). When the frequency was increased, the out-of-phase spectrum quickly decreased its relative intensity to that of the in-phase spectrum. This is consistent with the out-of-phase spectrum being that of slower relaxation: in Eqs. 2 and 3 the amplitude ratio $b_2(\omega)/b_1(\omega)$ is mathematically expected to become smaller as ω increases in the range of $k_1>\omega>k_2$.

In order to confirm the presence of a relatively faster heat releasing process and to determine its spectral shape $I_0(\lambda)A_1(\lambda)$, a trial spectrum for the faster process is tested in Fig. 4. Actually the trial spectrum is the in-phase spectrum at 35 Hz. In Fig. 4, the trial spectrum was so adjusted in its intensity to fit the long wavelength part of the mixture spectrum (the in-phase spectrum at 20 Hz) and was then subtracted from the latter. The difference between the mixed and the trial (the solid line in Fig. 4) reproduces the shape of the spectrum of the slower process which is actually the out-of-phase spectrum at 20 Hz. Therefore this trial spectrum is the spectrum of the faster process ($I_0(\lambda)A_1(\lambda)$ in Eq. 2).

The corrected spectra of the slower ($A_2(\lambda)$) and the faster ($A_1(\lambda)$) heat releasing processes are shown in Fig. 5. Their shapes are frequency independent but their relative intensities in the in-phase and out-of-phase spectra depend on the frequency.

Since the slower process is absent at 310 nm, we can determine the rate constant for the faster process by measuring phase lags ϕ_1 at 310 nm as a function of frequency. Figure 6 shows the results. It is seen in Fig. 6 that the curve calculated by using Eq. 6 with $\tau_s=0.2$ ms and $F/S=0.2$ fits the data well. The lifetime of the relaxed triplet state (T_1) of acetone has been reported to be 0.225 ms.[14] The expected values for F and S are 50 and 335 kJ mol^{-1} respectively for the relaxation path $S_1\rightarrow T_1\rightarrow S_0$ (excited at 310 nm). Therefore we assign the faster heat releasing process to

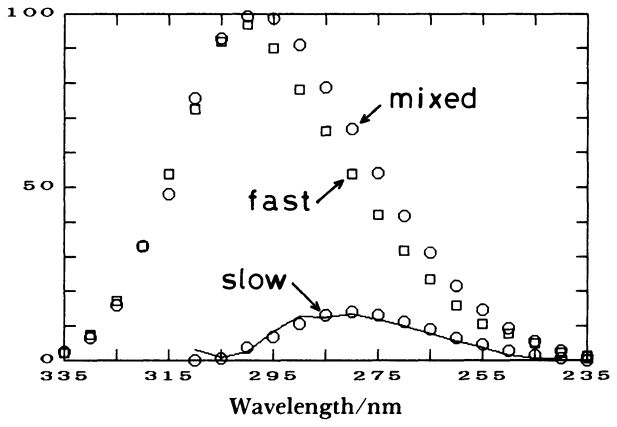

Fig. 4. Decomposition of the in-phase PA spectrum of Fig. 3 into a faster and a slower components. O (upper): the in-phase (ϕ=0°) PA spectrum in Fig. 3 (normalized to 100 at the peak).
□: trial spectrum for a faster component. O (lower): the out-of-phase (ϕ=90°) PA spectrum in Fig. 3 (height adjusted to fit the solid curve).
Solid curve: difference of O (upper) and □.

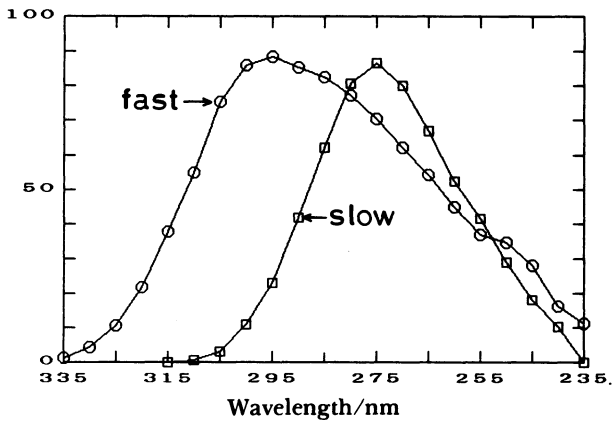

Fig. 5. Corrected PA spectra corresponding to the faster (T_1) and the slower (radicals) heat releasing processes. Normalized at their peaks. The correction was made by division with PA spectrum of carbon black.

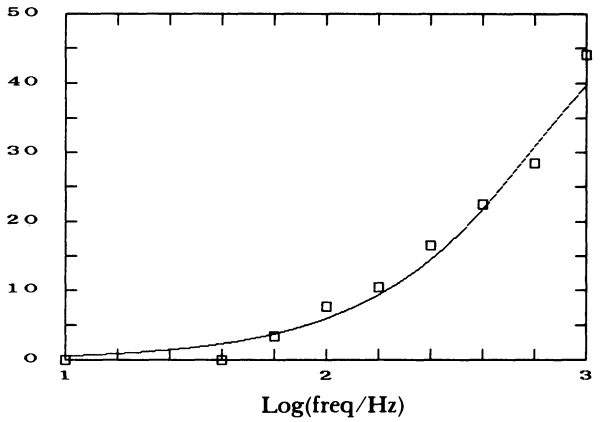

Fig. 6. Frequency dependence of phase lag of the heat released by T_1 observed at 310 nm.
Correction was made for the phase lag due to the apparatus. The solid line is the curve of Eq. 6 with $\tau_s=0.2$ ms and $F/S=0.2$.

the relaxation path via the triplet state (T_1).

On the other hand, the slower process can be assigned to the heat release on the recombination of radicals formed by photolysis of acetone because its heat releasing rate is slower than that of T_1 and its excitation wavelength ($\lambda<310$ nm) corresponds to the energy above the barrier height of decomposition, i.e. 385 kJ mol^{-1}.[14]

This slower process can not be studied directly in the same manner as the faster one, because its entire spectrum overlaps with that of the faster one. However, we can get some idea about the frequency dependence of the slower process indirectly from analyses of the PA spectra obtained at various frequencies. It should be mentioned here that in the following analysis of the slower process, we approximate second order recombination reactions by a pseudo first order reaction assuming a constant steady state concentration of the radicals.

We now know the spectral shape of the faster process $A_1(\lambda)$ and the slower $A_2(\lambda)$ as well as the phase lag of the faster process $\phi_1(\omega)$. We should therefore be able to determine $\phi_2(\omega)$ and $b_2(\omega)/b_1(\omega)$ of Eq. 1 by decomposing the in-phase spectrum into the two components (as done in Fig. 4) and comparing the resulting component spectra and the out-of-phase spectrum. To calculate the relative values of $b_2(\omega)$ from the ratio $b_2(\omega)/b_1(\omega)$, we used $b_1(\omega)$ calculated by using Eq. 5 with $F/S=0.2$ and $\tau_s=0.2$ ms for we did not measure $b_1(\omega)$. The calculated $b_1(\omega)$ is constant between 10 and 200 Hz and then gradually decreases down to 0.4 of the constant value as the frequency increases to 1000 Hz. The values of $\log\{b_2(\omega)\}$ and $\phi_2(\omega)$ thus obtained are shown in Fig. 7 (circles) as a function of $\log f$.

These curves are typical forms of the theoretical Eqs. 6 and 7; and are indications of the presence of two steps in the heat production process due to radicals. We estimate $F/S\lesssim 0.35$ from the highest and the lowest values of $\log\{b_2(\omega)\}$ and the approximate frequency of $\phi_2(\omega)$ peak of 35 Hz. These values lead to a very slow lifetime of $\tau_s\gtrsim 6$ ms. Equation 6 with these parameter values can reproduce the shape of $\phi_2(\omega)$ curve in Fig. 7 but predicts the peak of $\phi_2(\omega)\gtrsim 30°$. This discrepancy in the peak value of ϕ_2 may be due to the large errors in the determination of ϕ_2 by the spectrum subtraction method.

The two steps found in the heat production process due to radicals are interpreted as follows: heat release during the primary photodecomposition is the faster step remaining even at high frequencies ($f\leqq 100$ Hz) while the heat release on radical recombination is the slower one, present only at low frequencies ($f\leqq 20$ Hz).

PA Spectra in Air. PA spectra at 20 Hz with air as a buffer gas are shown in Fig. 8. As the PA spectra in Ar at 20 Hz (Fig. 3), these spectra also have two components. We decomposed the in-phase spectrum into a faster and a slower component spectra and found that the shapes of both component spectra were the same as those in Ar. Therefore we assign the out-of-phase spectrum to that due to radicals and the in-phase spectrum to a mixture of spectra due to radicals and to T_1.

The phase lags at 310 nm were found to be null in the frequency range of 10 to 1000 Hz. This indicates that the lifetime of T_1 is shortened (<20 μs) by the presence of about 100 Torr of O_2.

The frequency dependences of ϕ_2 and $\log b_2$ determined by spectral subtraction method as before are shown in Fig. 7 (squares). We used $\phi_1=0$ and $b_1=1$ for the heat production rate of T_1 in air because the rate is supposed to be much larger than that in Ar. A tail of a peak is observed in the ϕ_2 curve.

Therefore the heat production process due to radicals also has two steps: A faster one and a slower

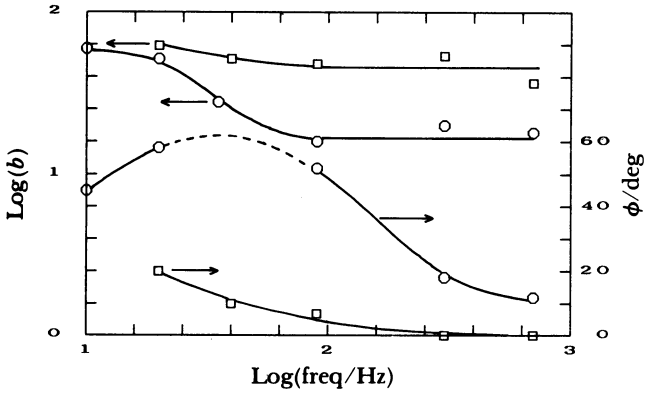

Fig. 7. Frequency dependences of PA signals due to the heat released by radicals.
O: Ar as a buffer gas, □: air as a buffer gas. ϕ: phase lag, b: amplitude. All the data were obtained indirectly from frequency dependence of spectral shape.

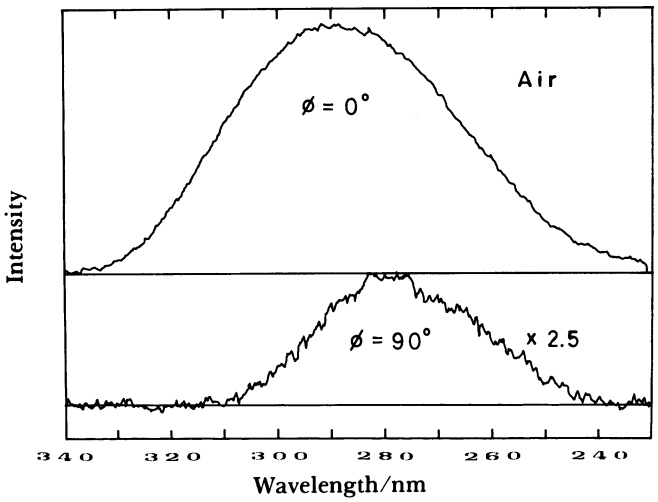

Fig. 8. PA spectra of acetone with air as a buffer gas (f=20 Hz).
Acetone 200 Torr and air 560 Torr. Phase angles are of relative values.

one. The faster step remaining at high frequencies (f>100 Hz) may be the primary photodecomposition and the reactions of the radicals so produced with O_2. For example, the pseudo first order rate constant of CH_3 with 100 Torr of O_2 is calculated to be 5×10^7 s^{-1} according to the literature.[19] The slower step observed at very low frequencies (f<20 Hz) could be heat release on recombination reactions of heavier radicals which are formed by addition of O_2 to primary radicals such as CH_3O_2.

Comparison of PA Spectra (PAS) with Absorption Spectra (ABS). In Fig. 9 the in-phase PAS at 423 Hz and the ABS with Ar as a buffer gas are compared. In Fig. 10 the in-phase PAS at 508 Hz and the ABS with air as a buffer gas are compared. The same sample was used in the measurements of the corresponding PAS and ABS. These PAS are corrected for $I_0(\lambda)$.

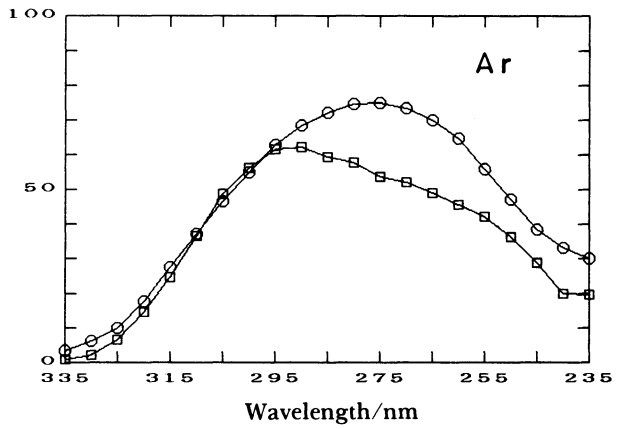

Fig. 9. Comparison of the absorption spectrum and the corrected PA spectrum of acetone with Ar as a buffer gas (f=423 Hz).
Acetone 200 Torr and Ar 560 Torr. The absorption-(O) is in % unit. PAS(□) is normalized to fit ABS at longer wavelengths.

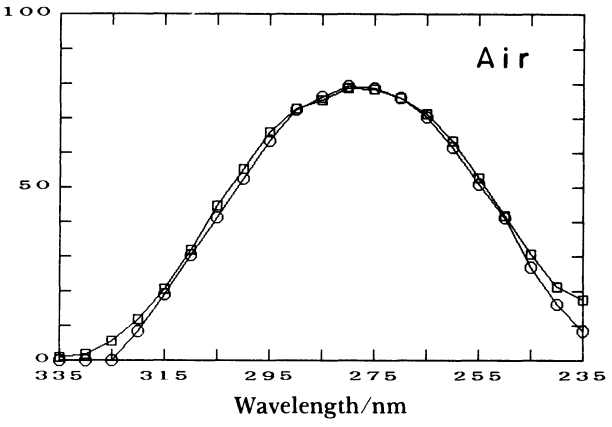

Fig. 10. Comparison of the absorption spectrum and the corrected PA spectrum of acetone with air as a buffer gas (f=508 Hz). See the legend of Fig. 9.

An ABS represents energy absorbed but a PAS represents energy released as heat. The heat defect in Fig. 9 can be considered due to failure to observe the slowly released heat at the high frequency.

The ABS in Fig. 10 as well as in Fig. 9 is proportional to $A(\lambda)$ in Eq. 2: $A(\lambda)=A_1(\lambda)+A_2(\lambda)$. The PAS in air (Fig. 10) can be also expressed by Eq. 2 as $A_1(\lambda)b_1(f=508)+A_2(\lambda)b_2(f=508)\cos(0)$. The effective heat at 508 Hz for T_1 path, i.e. $b_1(f=508)$ is equal to the total energy absorbed because the total energy of T_1 is released by the faster process in the presence of O_2: $b_1(508)$=430 kJ mol^{-1} at 280 nm. Judging from Fig. 7, $b_2(508)$ is the heat released by the faster process in the radical path: $b_2(508)=100+Q$ kJ mol^{-1} at 280 nm. Here the Q represents a sum of the heat released by the addition reactions of the two primary radicals to O_2. The coincidence of ABS and PAS in air (Fig. 10) requires Q to be about 330 kJ mol^{-1}.

Summary

It was found that there are two heat production paths in the 280 nm absorption band of acetone: one via T_1 and the other via radicals.

The spectral shapes for T_1 formation and photodecomposition were determined (Fig. 5).

The assignments of the heat observed in PA signals are summarized in Table 1 and the following reaction scheme.

$$S_0 \longrightarrow S_1$$
$$S_1 \longrightarrow T_1 + q_1$$
$$S_1 \longrightarrow \text{decomposition}(R_1+R_2) + q_2$$
$$T_1 \longrightarrow S_0 + q_3$$
$$R_1, R_2 \text{ recombination} \longrightarrow \text{products} + q_4$$
$$T_1 + O_2 \longrightarrow S_0 + O_2 + q_3' \quad (q_3=q_3')$$
$$R_1 + R_2 + 2O_2 \longrightarrow R_1O_2 + R_2O_2 + q_5$$
$$R_1O_2 + R_2O_2 \longrightarrow \text{products} + q_6$$

where q_i refers to heat released.

Table 1. Assignments of the Heat Observed[a]

Buffer	Path via T_1		Path via radicals	
	Fast	Slow	Fast	Slow
Ar	q_1 (50+α)	q_3 (335)	q_2 (50+α)	q_4 (335)
air	q_1+q_3' (385+α)	—	q_2+q_5 (385+α)	q_6

a) The numbers in parentheses are rough estimates of the amount of heat released in kJ mol^{-1} unit. $\alpha=1.2\times10^5/\lambda-385$ kJ mol^{-1}. λ is the excitation wavelength in nm.

References

1) K. Kaya, W. R. Harshbarger, and M. B. Robin, *J. Chem. Phys.*, **60**, 4231 (1974).
2) K. Kaya, C. L. Chatelain, M. B. Robin, and N. A. Kuebler, *J. Am. Chem. Soc.*, **97**, 2153 (1975).
3) M. B. Robin and N. A. Kuebler, *J. Am. Chem. Soc.*, **97**, 4822 (1975).
4) M. G. Rockley, *Chem. Phys. Lett.*, **50**, 427 (1977).
5) H. Nakamura, Y. Hiura, K. Tsubouchi, and N. Mikoshiba, *Jpn. J. Appl. Phys.*, **23**, L430 (1984).
6) T. F. Hunter, D. Rumbles, and M. G. Stock, *J. Chem. Soc., Faraday Trans. 2*, **70**, 1010 (1974).
7) T. F. Hunter and M. G. Stock, *J. Chem. Soc., Faraday Trans. 2*, **70**, 1022 (1974).
8) T. F. Hunter and M. G. Stock, *J. Chem. Soc., Faraday Trans. 2*, **70**, 1028 (1974).
9) T. F. Hunter and K. S. Kristjansson, *J. Chem. Soc., Faraday Trans. 2*, **78**, 2067 (1982).
10) T. F. Hunter, S. Lunt, and K. S. Kristjansson, *J. Chem. Soc., Faraday Trans. 2*, **79**, 303 (1983).
11) G. M. Breuer and E. K. C. Lee, *J. Phys. Chem.*, **75**, 989 (1971).
12) D. A. Hansen and E. K. C. Lee, *J. Chem. Phys.*, **62**, 183 (1975).
13) A. Gandini and P. A. Hackett, *J. Am. Chem. Soc.*, **99**, 6195 (1977).
14) R. A. Copeland and D. R. Crosley, *Chem. Phys. Lett.*, **115**, 362 (1985).
15) T. Heicklen, *J. Am. Chem. Soc.*, **81**, 3863 (1959).
16) $2CH_3 \rightarrow C_2H_6 + 335\ kJ\ mol^{-1}$, $2COCH_3 \rightarrow (CH_3CO)_2 + 293\ kJ\ mol^{-1}$.
17) H. J. Groh, G. W. Luckey, and W. A. Noyes, *J. Chem. Phys.*, **21**, 115 (1953).
18) W. R. Harshbarger and M. B. Robin, *Acc. Chem. Res.*, **6**, 329 (1973).
19) H. E. Van der Bergh and A. B. Callear, *Trans. Faraday Soc.*, **67**, 2017 (1971).